6th EASN International Conference

On Innovation in European Aeronautics Research

Chaired by Spiros Pantelakis & Mario Guagliano

Collection of Full Papers

easn

ANALYSIS AND OPTIMIZATION OF HYBRID POWERTRAINS FOR ROTOCRAFT APPLICATIONS

GIULIO AVANZINI, * ANGELO CARLÀ, AND TERESA DONATEO

Department of Engineering for Innovation, Università del Salento, Campus Ecotekne, Lecce, 73100, Italy
* *giulio.avanzini@unisalento.it*

Abstract

The use of a hybrid powertrain for a conventional single main rotor helicopter is investigated, with the objective of assessing its feasibility and its potential impact on improving safety, especially for single-engine rotorcraft. The study is focused on the characteristics of the powertrain and required battery pack. It is based on a simple analysis of power required in forward flight and the estimate of the total energy required for a powered landing maneuver after thermal engine failure. Current technologies are considered as well as expected improvements, especially as far as energy density and power density of the battery are concerned. The latter analysis is based on current trends for battery and motors technologies, in order to determine the technological breakthrough limit.

Keywords Hybrid rotorcraft; Hybrid powertrain; Helicopter safety.

1. Introduction

The paper aims at analyzing the viability of a hybrid powertrain for a conventional single main rotor helicopter configuration. Hybrid powertrains have the advantage of allowing the thermal engine (usually a turboshaft gas turbine in rotorcraft applications, although piston engines may also be considered) at their best efficiency, saving the excess power in a battery pack during flight phases that require less power, while relying on battery energy during (usually short) phases, when more power is required. As a further advantage, particularly relevant for single-engine rotorcraft, the battery pack should allow for a few minutes of endurance in case of engine failure. Instead of completing an autorotation descent with a critical engine-out landing, the residual energy in the batteries can be used for landing the rotorcraft by means of a more conventional (and inherently safer) powered landing sequence. These advantages need to be weighted against the increased weight and complexity of the resulting powertrain.

The concept has been the objective of some patents (e.g. Luyks, 2016; Harmon *et al.*, 2012; Waltner, 2016) and a few previous preliminary studies (Gurevich *et al*., 2014). Nonetheless, its viability still needs to be assessed, analyzing both instantaneous power balance and overall energy balance over the entire mission. Such an analysis allows one to evaluate if weight penalties associated to the hybrid powertrain (the presence of a battery pack coupled with large electric generator and engine) are worth the advantages in terms of better overall efficiency and increased safety.

The trend towards an increasing "electrification" of all classes of aircraft is a well-established one. In the last decades, the use of fly-by-wire and fly-by-light control systems, the increased level of automation, with redundant on-board computers and sensors, and, more recently, the use of electrical actuators which are replacing traditional hydraulic ones, resulted in more demanding electrical systems, well beyond the classical needs for pumps, lights, and air conditioning. Little more than 20 years ago Abzug and Larrabee wrote that "fully electrical airplane flight control systems are a possibility for the future" (Abzug and Larrabee, 1994, p. 83). At the time, the term "all electric aircraft" referred to the control system only. They did not even considered the possibility of hybrid powertrains for aeronautical applications, let alone a fully electrically powered airplane. Nowadays, there are several designs of prototypes, some of which at an advanced testing stage, that successfully demonstrated the concept of hybrid powertrain for fixed-wing aircraft (such as the experimental E-Fan 1.2 hybrid electric airplane built by Airbus). Fully electrical aircraft are still at a prototype development stage. Among the most advanced concepts of fully electric aircraft, we only cite here the NASA X-57 experimental aircraft, which is expected to perform its maiden flight during 2017.

In fixed-wing aircraft application, the hybrid electric concept can be used to increase safety, reduce noise by means of electric flight at takeoff and landing, to improve range and endurance, to minimize fuel consumption (Merical *et al.*, 2014; Harmon, 2016; Friedric *et al.*, 2014, Greiser *et al.*, 2011). As a consequence, together with the development of experimental test-beds, also flight mechanics analysis tools and design techniques need to be developed for tackling the challenge of sizing a hybrid or a fully electric aircraft. As an example, the classical Breguet equations for the determination of aircraft range and endurance performance are being reconsidered by the scientific community, in order to take into consideration these innovative propulsion system configurations (Traub, 2011; Avanzini and Giulietti, 2013). The resulting equations are at the basis of a novel set of sizing tools for small-scale fixed wings unmanned aircraft, for the definition of optimal battery pack for a given type of payload (Avanzini *et al.*, 2016a).

Electrical propulsion is extremely popular for many small-scale rotorcraft, such as light helicopter models and multi-rotor platforms. Unfortunately, with current battery technologies, small-scale electric rotorcraft pay a significant price in terms of endurance, which seldom approach a limit of 30 minutes, but is usually in the range of 10 to 15 minutes (Gatti *et al.*, 2015). In the case of full-scale vehicles, rotorcraft appear to be less prone to viable engineering solutions for an operational prototype featuring a fully electrical propulsion system, because of the high level of power required and the weight of the battery system, even considering the most advanced type of Li-Po batteries. On the converse, the wide variation of power required in different flight conditions may provide an interesting scenario for the application of a hybrid powertrain. The objective of the present paper is thus to investigate the possibility of developing a hybrid powertrain for full-scale manned rotorcraft, mainly aimed at improving flight safety of single-engine helicopters. The analysis is performed by means of a Matlab model of the proposed powertrain and a sizing procedure based on literature data for batteries and motors.

Two different mission profiles are considered: a simple transport mission and a search-and-rescue (SAR) mission profile. In the first simpler scenario, the helicopter is required to cover a given distance at cruise speed between the takeoff and the landing sites. In the second case, the helicopter is required to reach the operation area at high speed, perform operations assimilated to hovering at low altitude, and return to the base. An elementary model is adopted for estimating power absorbed by main and tail rotor and on-board systems during the mission. Emergency landing procedures are simulated and the corresponding power request is used to size an electric path (motor+driver+battery) that could replace the existing second engine while providing the necessary redundancy. To this end, the electric path was sized in order to keep the same mass of the replaced engine (150 kg). The investigation is initially performed with state of the art technologies for batteries and motors. However, technological trends for high-performance batteries and motors are also investigated and the minimum requirements in terms of power density and energy density are calculated.

The paper is organized as follows. A review of the architecture of hybrid powertrains for aeronautical application is provided in the next section, highlighting those aspects that appear as relevant or even critical for the rotorcraft case. The definition of power required and energy consumption in various operational scenarios is discussed in Section 3. Methods for sizing the elements of the hybrid powertrain are then reviewed in Section 4. Section 5 provides some results. The final section summarizes the conclusions of the study.

2. Hybrid powertrains and their aeronautical applications

Hybrid Electric Propulsion Systems (HEPS) are characterized by the use of two energy storage systems, usually a fuel tank and a battery. In the presence of batteries it is possible to optimize the operating point of the engine, which can also be downsized. Engines are usually designed to meet the requirements of maximum thrust and/or power at takeoff or maximum speed, but as a matter of fact the largest portion of the mission (*i.e.* the cruise segment), requires a reduced throttle setting and the engine does not work at its maximum power level.

HEPS can be classified into parallel and series powertrains. In the case of series configurations, the mechanical drive path that moves the propeller is connected to an electric motor while the internal combustion engine is used to drive a generator. The electric power to the motor is the algebraic sum of the battery power and the engine/generator power. The series configuration is suitable for low-speed, high-torque applications but it is less efficient than the parallel one, where both the engine and the motor are mechanically connected to the drive train. Moreover, it requires larger batteries and electric machines.

2.1. *Fixed wing applications*

HEPS for UAVs were studied numerically in literature (Merical *et al.*, 2014; Harmon, 2016; Friedric *et al.*, 2014) and tested experimentally in (Greiser *et al.*, 2011). A test flight was performed with a hybrid electric aircraft [1] and a reduction of fuel consumption of 30% with respect to the conventional gasoline engine was estimated. A limited amount of information was released on the powertrains adopted. Unfortunately, HEPS increase overall propulsion system complexity. Moreover, HEPS are mode demanding in terms power plant mass and volume, both critical aspects in aircraft design, where reliability and power density are the main goals.

2.2. *Rotary wing applications*

In helicopter applications, the use of electric drive guarantees several advantages including:

- Flexibility and maneuverability thanks to the possibility of adjusting the rotation speed of the rotor;
- High reliability and improved maintenance workability;
- Lower emissions and noise.

Some examples of electric and hybrid helicopters have been presented in literature. The possible variants in terms of powertrain configurations were summarized in Gurevich *et al*. (2014). The electric drive can be used for the tail rotor only or for both rotors, with both parallel and series schemes.

3. Power required and energy consumption in various operational scenarios

The analysis is based on a helicopter configuration taken from available data for the Agusta-Westland A109 helicopter, a lightweight, twin-engine rotorcraft used in various roles, such as light transport, search-and-rescue, and military roles. In the case of single-engine failure, the twin-engine configuration allows a power reserve to perform an emergency landing. The idea behind the study is to evaluate the possibility of replacing the second engine with an auxiliary electric power unit, thus obtaining a hybrid electric powertrain, which should allow for significant savings in terms of fuel consumption. At the same time, the need for an autorotation maneuver in case of engine failure should be circumvented by exploiting the battery charge for an electrically powered landing, thus increasing safety of the helicopter with respect to an equivalent single engine configuration.

3.1. *Helicopter model*

The study requires the evaluation of power required in flight at various flight conditions and an estimate of the total energy required for performing the electrically powered emergency landing. These data are at the basis of the process of sizing the electric drive and the battery pack necessary.

The analysis of the power required along the considered mission profiles was performed by means of a very simple set of tools implemented in a Matlab program. The characteristics of the mission profile are defined first in terms of distance covered, cruise altitude h, velocity profile V and climb and descent angles γ during the terminal phases of the transport mission. For the SAR mission a descent and a loiter phase in the operational area were added, assuming that the vehicle is expected to return to the same base after performing its task.

Once the mission profile is known, the required power at each point along the trajectory can be evaluated. Following the approach presented in McCormick (1995), required power P_R is split into its main contributions:

$$P_R = P_P + P_{MR} + P_{TR} + P_C + P_S \tag{1}$$

where

- $P_P = DV$ is parasite power, which is proportional to helicopter fuselage drag, $D = \frac{1}{2}\rho V^2 SC_D$, where ρ is air density and the product SC_D is referred to as the equivalent flat plat parasite area; the parasite power is thus proportional to V^3;
- P_{MR} and P_{TR} are main and tail rotor power, respectively;
- $P_C = WV\sin\gamma$ is climb power, proportional to helicopter weight W and climb rate, $\mathrm{d}h/\mathrm{d}t = V\sin\gamma$;
- P_S is power required by on-board systems.

Main rotor power is the sum of two terms,

$$P_{MR} = P_{ind} + P_{pr} \tag{2}$$

[1] http://sustainnovate.ae/en/industry-news/detail/hybrid-electric-airplane-takes-flight, retrieved on-line on October, 30th 2015.

In the framework of momentum theory, induced power P_{ind} is equal to the ideal power, $P_{id} = T w_i$, given by the product of total rotor thrust

$$T = 2\rho(\pi R^2)\, V_D w_i \tag{3}$$

and induced speed w_i, where R is rotor radius and velocity at the disk V_D is equal to

$$V_D = \sqrt{\left(V\sin\alpha - w_i\right)^2 + \left(V\cos\alpha\right)^2} \tag{4}$$

Total rotor thrust and induced velocity are determined from the current flight condition. Helicopter translational dynamics satisfy the equations of motion

$$\begin{aligned} \frac{W}{g}\frac{dV}{dt} &= -T\sin\alpha - D - W\sin\gamma \\ \frac{W}{g}V\frac{d\gamma}{dt} &= T\cos\alpha - W\cos\gamma \end{aligned} \tag{5}$$

If $V(t)$ and $\gamma(t)$ are known functions of time, it is possible to solve the system provided by equations (3) and (5) with respect to T , α and w_i (taking into account equation (4)). The solution requires a simple iterative scheme, which converges after few iterations (McCormick, 1995). Provided that momentum theory only accounts for velocity increments in the axial direction (whereas a real rotor is characterized by a more complex wake), induced power is often written in the form $P_{ind} = 1.15\ P_{id}$, where the empirical coefficient 1.15 accounts for the dissipation due to tangential and radial velocity increments, not accounted for in this elementary model.

Profile power P_{pr} is obtained from blade element theory considerations, in the form

$$P_{pr} = \left(\rho\pi\Omega_{MR}^2 R^4\right)\frac{\sigma\bar{C}_d}{8}\left(1+3\mu^2\right) \tag{6}$$

where Ω_{MR} is main rotor angular rate, $\sigma = N_b c/(\pi R)$ is rotor solidity (with N_b number or rotor blades and c rotor blade chord), C_d is rotor blade airfoil average drag coefficient, and finally $\mu = V/(\Omega R)$ is the advance ratio. Tail rotor power is evaluated with the same approach, substituting in equations (3), (4), and (6) the values of tail rotor thrust T_{TR} (obtained from helicopter equilibrium around the yaw axis) and the geometric, kinematic and aerodynamic characteristics of the tail rotor (radius, chord, angular rate, average drag coefficient, solidity, etc.).

The modeling approach adopted here, derived with minor modifications from McCormick (1995), is simple and, apparently, potentially inaccurate in critical flight condition, but helicopter high level modeling, which include a more accurate representation of rotor and fuselage aerodynamics, is required only when demanding maneuvering tasks are considered (Avanzini *et al*., 2016b). Only smooth mission profiles are dealt with here, and modeling accuracy is adequate for the preliminary sizing of a HEP that needs to assess its technological feasibility.

3.2. *Operational scenarios considered in the analysis*

A transport mission with an altitude of 300 m and a cruise speed of 78 m/s is considered. The transport mission is assumed to be interrupted at a certain point by an engine failure. The emergency landing is then started. The profile mission and the two starting points considered here are shown in Fig. 1. When point A along the mission profile is considered, engine failure occurs during the cruise phase. This was chosen as worst-case scenario because the helicopter flies at a velocity close to its maximum airspeed limit. Conversely, at point B, the helicopter is starting the approach and landing sequence and airspeed is reduced.

In the emergency landing, the helicopter performs three phases:

1) a forward flight phase for approaching the landing site with a prescribed descent angle (FF),
2) a vertical approach (VA)
3) a short hovering phase (H).

For each phase, some parameters need to be defined to generate the landing profile, namely final speed, final altitude, descent angle and the duration τ of the phase.

A second mission scenario was considered, that is, a SAR mission in a mountain environment, where the flight distance is shorter, but the helicopter is required to climb up to the altitude of the operational area. As a matter of fact, and in spite of the more demanding altitude gain, the engine failure scenarios along this mission appear less demanding (thus less critical) in terms of total energy required for completing the emergency landing sequence. Provided that battery weight is the most critical aspect in sizing the HEP, this case is not reported for the sake of conciseness.

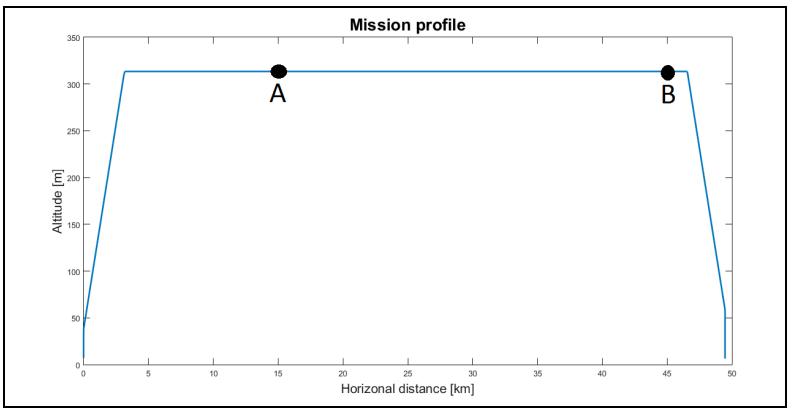

Fig. 1. Selected starting points for emergency landing during the transport mission

4. Sizing of the electric drive

The electric drive was designed with the constraint of a total mass (battery + motor + driver) equal to the mass of the second engine to be replaced by the electric drive. Literature correlations for battery, motor and driver were used to estimate their mass as reported in the next paragraphs.

4.1. *The battery*

In the present model, commercial Lithium polymer batteries were chosen as representative of current technology. Table 1 shows the specifications of a lithium polymer cell that has a nominal energy density of approximately 140 Wh/kg. A battery module is obtained by connecting a large number of cells in series and parallel, to achieve the desired values of bus voltage and capacity (energy). However, the mass of the battery pack M_{batt} is larger than the sum of cells in parallel and/or in series because of the presence of inter-cell connectors, separators infra-cell, control units, etc. that account for at least 30% of the final mass (Arista *et al.*, 2015). The additional mass is also increased when higher discharge current are required. Consequently, the actual energy density at a battery-pack level is much lower than the cell energy density.

Using data of different Li-Po batteries tested at CNR-Italy (Arista *et al.*, 2015), empirical correlations were derived for mass and volume of the battery pack as a function of nominal capacity (in Ah) and number of cells in series (Fig. 2). For a battery with a nominal capacity of 40 Ah and 73 elements in series, this correlations give reasonable values of 86 Wh/kg for energy density and 210 Wh/liter for volumetric energy density.

Power density of the battery pack depends on the maximum continuous current in discharge that can be increased either increasing the capacity or increasing the maximum continuous discharge current[2]. In the second case, the energy density is expected to decrease due to the higher mass required to sustain higher currents. Note that energy density of lithium batteries is expected to increase up to 1700 Wh/kg within the next 10 to 20 years (Hepperle, 2012) and higher maximum continuous currents are already becoming available nowadays. Moreover, the volumetric energy density is also expected to improve (Gallaugher *et al.,* 2016). For these reasons, different scenarios of future reasonable battery development were considered in the present investigation.

Table 1. Technical specifications of storage technology (Li-Po)

Parameter [Unit]	Value
Rated Cell Voltage [V]	3.7
Max Cell Voltage [V]	4.2
Cut-off Cell Voltage [V]	2.7
Max continuous current in discharge	$5C_{nom}$
Peak current	$10C_{nom}$
Max continuous current in charge	$2.2C_{nom}$
Operating temperature [°C]	-20/60

[2] http://www.lipolbattery.com/

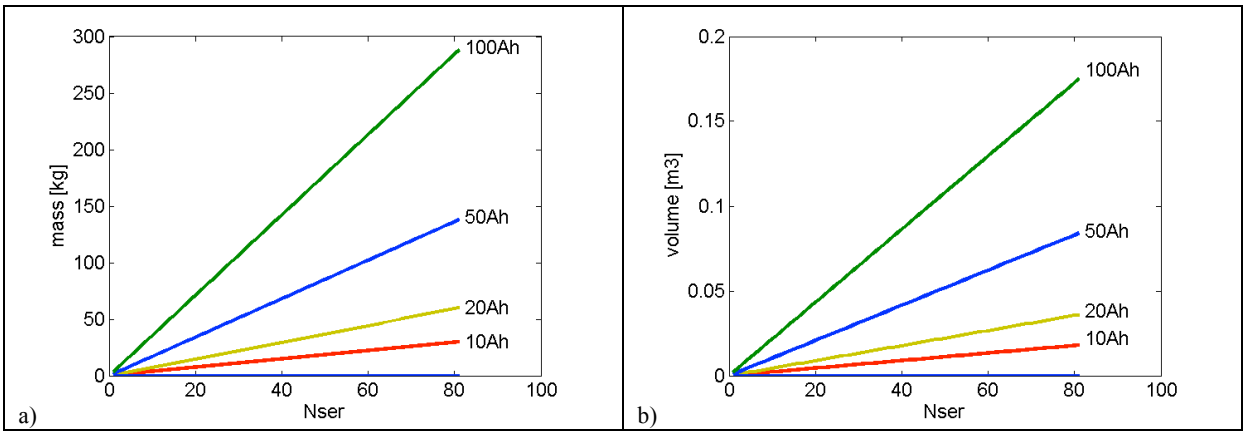

Fig. 2. Mass and volume of batteries versus number of elements in series and nominal capacity

4.2. *The electric drive*

For a specified motor technology, gravimetric and volumetric power densities of motors and efficiency depend on machine size and speed. Liquid cooled permanent magnet brushless DC motor drives were considered in the present investigation as representative of current technology (Hendershot *et al.,* 1994). The peak power is assumed to be 2.5 times the nominal power (Hendershot *et al*. 1994). However, the motor peak power is limited by the available battery peak power.

Nominal efficiency of the motor, η_M, increases when nominal power and rotational speed increase. To take into account the whole electric drive (motor and inverter), the efficiency of the motor is multiplied by the efficiency of the inverter, which increases with bus voltage. Extrapolating the experimental data reported by Geng *et al.* (2013), the following dependence of inverter efficiency on bus voltage was implemented:

$$\eta_{\text{inv}} = \frac{95.4 + 0.0026 V_{bus}}{100} \tag{7}$$

The overall efficiency of the electric drive for a V_{bus} of 270 V is shown in Fig. 4. It ranges from 0.95 for a 50 kW motor to 0.97 for a 500 kW machine rotating at 10000 rpm, whereas it decreases to approximately 0.9 at 2000 rpm. Note that larger rotational speeds require the use of heavier gearboxes for the connection of the motor with the rotor, thus leading to an increase of mass, volume and complexity. For this reason a speed of 2000 rpm was considered in the present investigation, in spite of the reduced value of electric drive efficiency.

Mass and volume of the motor are calculated from its nominal power and speed with the sizing technique proposed in Hendershot *et al.*(1994). Note that mass to torque and volume to torque ratios of electric motor decrease with size. The mass of the whole electric drive is obtained by summing up the mass of the motor and the mass of the inverter. Electric drive mass expressed in kg is estimated as follows:

$$M_{\text{ED}} = M_{\text{M}} + 0.339 P_{M,nom} + 5.45$$

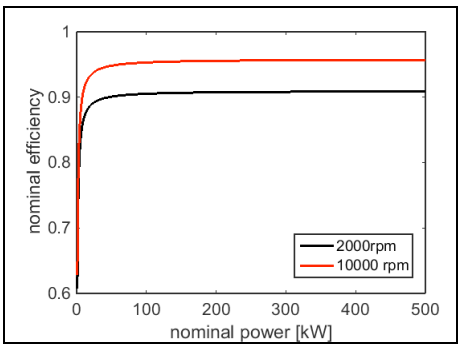

Fig. 3. Efficiency of the electric drive as a function of the nominal electric power at 2000 and 1000 rpm (V_{bus}=270V)

The volume in liters of the whole electric drive is given by:

$$Vol_{\mathrm{ED}} = Vol_{\mathrm{M}} + 0.57P_{M,nom} + 7.94$$

where $P_{M,nom}$ is the nominal power of the motor expressed in kW and $T_{M,nom}$ is its nominal torque expressed in Nm. The overall gravimetric and volumetric power densities of the electric drive as a function of nominal power and speed are shown in Fig. 4. In the present investigation the speed of the motor was set equal to 10000 rpm to avoid the usage of a bulky gearbox. Possible developments in the motor power density were also considered in the present investigation (Hepperle, 2012).

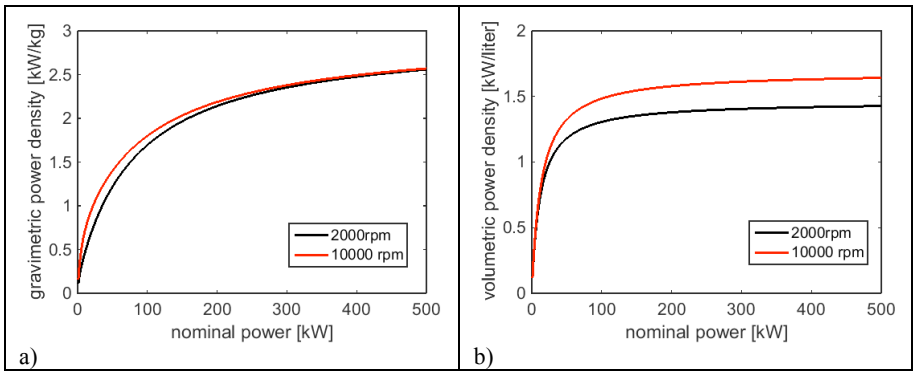

Fig. 4. Gravimetric and volumetric power densities of the electric drive versus its nominal power at 2000 and 10000 rpm

4.3. *The scenarios*

The emergency landing maneuver of Fig. 5 with a descent angle of 5° requires a brake power ranging from 200 to 515 kW, with an average of 394 kW. The integral of the curves of required power provides an estimate of the required mechanical energy, which is equal to 7.3 kWh. Once divided by electric drive efficiency, these values give the power and the energy that needs to be generated by the batteries to fulfill the proposed mission task. The nominal power of the battery depends on both the number of elements in series and the nominal capacity (that influences the maximum current in discharge as already explained). Therefore, there are two degrees of freedom in sizing the battery: increasing the nominal capacity or increasing the number of elements in series.

In the present investigation the bus voltage was initially set equal to 270 V as proposed in literature (Bérubé *et al.*, 2011), but increased to 540 V in the development scenarios to account for the large power required for the emergency landing. Accordingly, 73 and 143 elements in series were considered, respectively for the 270 V and 540 V scenarios. The nominal capacity was adjusted with iterative procedure in the attempt to match the energy and power request of emergency landing with the constrain of $M_{batt}+M_{ED}$ = 150 kg (with a margin of ±5 kg).

Four scenarios were considered (see Table 2 and Fig. 6). The first one considers the use of available technology, *i.e.* commercial Li-po batteries and permanent magnet motors, as illustrated in Section. The mass constrain limits the battery capacity to 40 Ah. Scenario 2 assumes data coherent with expected development for batteries and motors in 2040, as reported by Hepperle (2012). In particular battery energy density is increased by a factor 11, power density from 0.4 to 19 kW/kg and from 1.7 to 5.4 kW/kg for battery and motor, respectively. The improved energy density allows the nominal capacity to be increased up to 60Ah while keeping the overall mass within the constraint value. In this scenario the mass of motor and drive accounts for 78% of the overall mass (Fig. 6).

Scenarios 3 and Scenario 4 consider the minimum improvement required in terms energy density and power density, respectively, sufficient for matching the requirement of the emergency landing. More specifically, Scenario 3 considers an improvement of battery in terms of Ah/kg. Consequently both the power density and the energy density are increased with respect to today's technology while the motor power density is from today's technology (Fig. 4). Scenario 4 considers the same Ah/kg for the battery but predicts an improvement in both battery power density (by increasing the max continuous and peak current) and motor power density. The availability of power and energy for emergency landing with the four scenarios is compared with the requirements of the emergency landing in Table 3.

Values for continuous and peak power were calculated by multiplying bus voltage and continuous/peak current, respectively. These values of power where properly reduced to take into account the efficiency of the electric driveline. The available energy was obtained by multiplying nominal capacity and bus voltage. Note that, in this simplified analysis, the effect of variable discharge current on actual battery capacity is not considered. With state of the art technology considered in Scenario 1 it is not possible size an electric drive that allows for completing the emergency landing. Available peak power and continuous power are both well below the required values. The electric drive of Scenario 2 is, on the other hand, quite oversized, both in terms of power

and energy. Scenario 3 is the most suitable for power request, but the available energy is still higher than the required one, thus resulting in a suboptimal design. It is evident from these results that increasing power density is more critical than increasing energy density for this type of application. Scenario 4 was chosen in order to fulfill the request of power and energy, with a margin that takes into account the efficiency of the electric path and the effect of variable discharge current on actual battery capacity.

Recently, Siemens[3] developed an electric motor for aircraft application with a nominal power of 260 kW, a bus voltage of 560 V and a power density of 5 kW/kg.. Data in literature show that power density up to 11 kW/kg can be obtained with lithium batteries (Nagata *et al.*, 2014; Zhang *et al.*, 2016) even if with relatively low energy density (up to 49 Wh/kg). This means that Scenario 3 and 4 will be achievable in a few years. As for the volume occupied by the electric system (Fig. 7), state of the art technology of Scenario 1 requires a total volume of about 90 liters, whereas about 300 liters are required for Scenario 4 (because of the poor volumetric density of current motors). As seen for mass, also volume required is mainly occupied by the motor. Since an improvement of a factor 4 in the volumetric density of the motor[3] has been already achieved, the total volume for Scenario 4 would be less than100 liters, even with state of the art volumetric density of the battery.

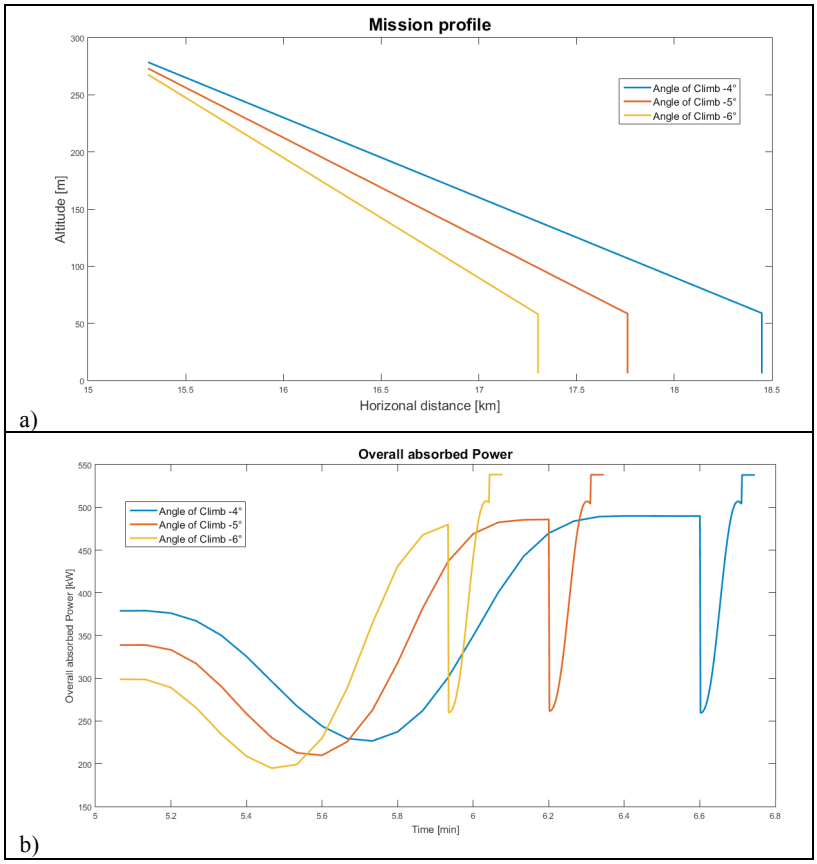

Fig. 5. Sensitivity analysis with respect to the descent angle

Table 2. Battery and motor development scenarios

Nominal values [Unit]	Scenario 1	Scenario 2	Scenario 3	Scenario 4
Capacity [Ah]	40	60	30	18
Bus Voltage [V]	270	540	540	540
Max continuous current [A]	$5C_{nom}$	$20C_{nom}$	$20C_{nom}$	$50C_{nom}$
Peak current [A]	$10C_{nom}$	$40C_{nom}$	$40C_{nom}$	$100C_{nom}$
Pack-level battery energy density [Wh/kg]	86	948	437	150
Pack-level battery power density [kW/kg]	0.4	19	8.8	7.5
Motor power density [kW/kg]	1.7	5.4	2.5	4.6

[3] www.siemens.com/press/pool/de/feature/2015/corporate/2015-03-electromotor/factsheet-erstflug-weltrekordmotor-d.pdf

Table 3. Available and required values of power and energy

	Available				**Required**
	Scenario 1	Scenario 2	Scenario 3	Scenario 4	**for emergency landing**
Peak power [kW]	104.7	1257.4	628.6	916.8	**515**
Continuous power [kW]	52.35	628.7	314.3	458.4	**394**
Energy [kWh]	10.8	32.4	16.2	9.45	**7.3**

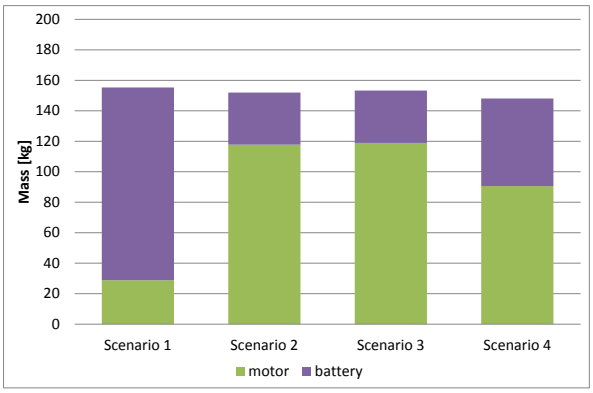

Fig. 6. Mass distribution in the four scenarios

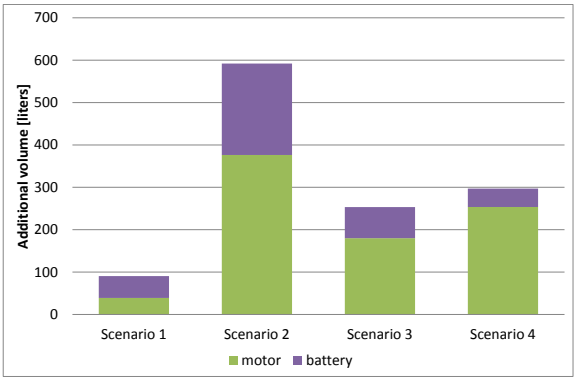

Fig. 7. Additional volume required by the proposed scenarios with today's volumetric densities

5. Simulation of the emergency landing

To verify the capability of the proposed system in fulfilling the requirements of the emergency landing, the power request $P_{prop}(t)$ calculated with the helicopter model is used as input for the model of the electric path. The electric power to be produced by the battery at any time is calculated as:

$$P_{batt}(t) = \frac{P_{prop}(t)}{\eta_M \eta_{inv}} \tag{2}$$

The current $I(t)$ is then obtained as

$$I(t) = \frac{P_{batt}(i)}{V(i)} \tag{3}$$

where battery voltage at time t is a function of open circuit voltage V_{OC}, that, in turn, depends on the state-of-charge (SOC) of the battery, i.e. its remaining capacity expressed as a percentage of the nominal capacity:

$$V(t) = V_{OC}(t) - R \cdot I(t) \tag{4}$$

The open circuit voltage is calculated as the sum of three terms: a constant voltage E_0, a polarization term and an exponential loss (Tremblay *et al.*, 2007):

$$V_{OC}(t) = \mathrm{E}_0 - \frac{100 \cdot \mathrm{K_b}}{\mathrm{SOC}(t-1)} + \mathrm{A} \cdot \exp\left[-B \cdot C_{nom}\left(1 - \frac{SOC(t-1)}{100}\right)\right] \quad (5)$$

The values of the parameters R, E_0, A, K_b and B depend on the battery technology. Their values for the Li-Po batteries were obtained by fitting experimental data (Arista *et al.*, 2015) and are reported in Table 4. The same parameters were assumed for all the scenarios considered in the present investigation. SOC of the battery was set equal to 100% at the beginning of the simulation. Then, it is calculated with an improved version of the Coulomb counting method that takes into account the capacity reduction when the battery is discharged with currents different form the nominal C-rate (1C for the LiPo batteries) (Leksono *et al.*, 2013), by introducing a pseudo-effective current Ieff, (Hausmann *et al.*, 2013) defined as:

$$I_{eff} = I\left(\frac{I}{I_{nom}}\right)^{nb-1} \quad (6)$$

where n_b is the Peukert coefficient that depends on temperature, concentration of the electrolyte and structure of the batteries (Su *et al.*, 2008). I_{nom} is the current at which the nominal capacity is referred to (1C). The values of Peukert coefficient for Li-Po batteries is assumed n_b= 1.05, according to what is reported in Arista *et al.* (2015). The SOC is then calculated as

$$\mathrm{SOC}(t) = \mathrm{SOC}(t - \Delta t) - 100 \cdot \frac{I_{eff}(t)}{C_{nom}} \Delta t \quad (7)$$

Table 4 – Coefficients of the Li-Po model

Parameter [unit]	Value
E_0 [V]	3.7
Kb [V]	0.00078
A [V]	0.5458
B [$(Ah)^{-1}$]	0.1000
n_b	1.05

The internal resistance of the model is tuned by matching the maximum continuous discharge current for each scenario. To take into account different scenarios, the internal resistance was assumed inversely proportional to the max discharge current. The state of the charge of the battery during the emergency landing is shown in Fig. 8 for scenarios 2-4 (it could not be calculated for scenario 1 due to the insufficient battery power). As already shown in the sizing section, the energy content of batteries in scenarios 2 and 3 is much larger than what is actually required. In fact, the battery is still charged at 80% in Scenario 2 and 50% in Scenario3. In the last case, the system is sized to match the request of energy thus the battery is fully discharged at the end of the landing.

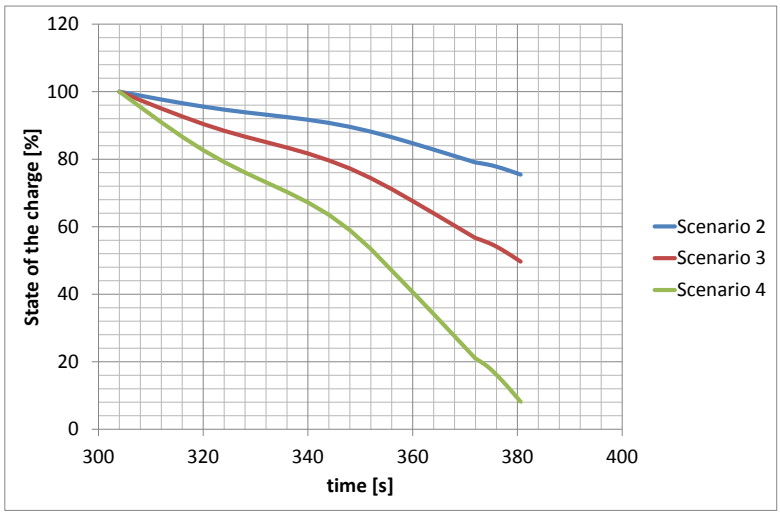

Fig. 8. Time histories of state of the charge for scenarios 2-4

6. Conclusions

The paper analyzed the feasibility of a hybrid electric powertrain for application in the framework of single-main rotor single-engine light helicopters. The work was aimed at sizing the electric drive (engine and batteries in particular), that allow an electrically powered emergency landing to be successfully completed after thermal engine failure. The analysis performed demonstrates that, with current technologies, the design of a hybrid helicopter is still unfeasible, although projection of trends in energy and power densities of both electric motors and batteries suggests that a viable solution may be obtained within few years.

References

Abzug M.J. and Larrabee E.E. (1997). *Airplane Stability and Control: A History of the Techologies that Made Aviation Possible*, Cambridge Univ. Press, Cambridge (UK).

Arista A., Ferraro M., Sergi F., Antonucci V. (2015). Dynamic Model of High-Performance Li-ion cells (LiFePO4, Li-Polymers and LiFP6 NBC) in different load conditions. 6th IC-EpsMsO, Athene, ISSN: 2241-9209.

Avanzini G. and Giulietti F. (2013). Maximum Range for Battery-Powered Aircraft, *J. of Aircraft*, **50**(1):304-307.

Avanzini G., de Angelis E.L. and Giulietti F. (2016a). Optimal Performance and Sizing of a Battery-Powered Aircraft. Accepted for publication on *Aerospace Science and Technologies.*

Avanzini G., De Matteis G., and Torasso A. (2016b). Assessment of Helicopter Model Accuracy Through Inverse Simulation. Accepted for publication on *Journal of Aircraft*, available on-line since July 29, 2016, doi: 10.2514/1.C033847

Bérubé D., Dessaint L. A., Liscouet-Hanke S., Lavoie C. (2011). Simulation of a hybrid emergency power system for more electric aircraft. Canadian Aeronautics and Space Journal, **57**(3): 155-162, 10.5589/q11-018

Friedrich, C. and Robertson, P.A., (2014). Design of a hybrid-electric propulsion system for light aircraft. 14th AIAA Aviation Technology, Integration, and Operations Conference.

Gallagher K.G., Trask S. E., Bauer C S, Woehrle T., Lux S. F., Tschech M., Lamp P., Polzin B J, Ha S., Long B., Wu Q., Lu W., Dees D. W., Jansen A. N. (2016). Optimizing Areal Capacities Through Understanding The Limitations Of Lithium-Ion Electrodes. Journal of The Electrochemical Society, 163 (2) A138-A149.

Gatti M., Giulietti F. and Turci M. (2015). Maximum endurance for battery-powered rotary-wing aircraft, *Aerospace Science and Technology*, **45**:174–179.

Geng P., Wu W., Huang M. , Blaabjerg F. (2013). Efficiency Analysis on a Two-level Three-Phase Quasi-Soft-Switching Inverter",. Twenty-Eighth Annual IEEE Applied Power Electronics Conference and Exposition (APEC), 2013, pp. 1206 - 1212, DOI: 10.1109/APEC.2013.6520452.

Greiser C.M., Mengistu, I. H., Rotramel T. A., Harmon F.G., (2011). Testing of a Parallel Hybrid-Electric Propulsion System for use in Small Remotely-Piloted Aircraft. AIAA 2011-5903, 9th Annual International Energy Conversion Engineering Conference, 31 July – 3 August, San Diego, California, 2011.

Gurevich O., Lukovnikov A., Gulienko A. Zakharchenko V., Kovalenko I., Suntsov. P. (2014). Analysis of possibilities to apply electric technologies for helicopter propulsion system. 29th Congress of the International Council of the Aeronautical Sciences. St. Petersburg, Russia, September 7-12, 2014.

Gurevich O., Lukovnikov A., Gulienko A., Zakharchenko V., Kovalenko I., and Suntsov P. (2014). Analysis of Possibilities to Apply Electric Technologies for Helicopter Propulsion System. *Proceedings of the 29th Congress of the International Council of the Aeronautical Sciences (ICAS 2014)*, St. Petersburg, Russia, September 7-12, 2014, **4**: 2864-2869.

Harmon F. H. (2006). Conceptual Design and Simulation of a Small Hybrid-Electric Unmanned Aerial Vehicle. Journal of Aircraft, Vol. 43, No. 5.

Harmon F.G., Hiserote R. M., Rippl M. D., Ausserer J. K. (2012). Parallel Hybrid-Electric Propulsion Systems for Unmanned Aircraft. Patent Application No. US 2012/0209456, Aug. 16, 2012.

Hausmann A., Depcik C. (2013). Expanding the Peukert equation for battery capacity modeling through inclusion of a temperature dependency. *Journal of Power Sources*, **235**: 148-158, doi:10.1016/j.jpowsour.2013.01.174.

Hendershot J. R., Miller T., (1994). Design of Brushless Permanent-magnet Motors, Magna Physics Pub.

Hepperle M. (2012) Electric flight: Potential and limitations. *In AVT-209 Workshop on ENERGY EFFICIENT* TECHNOLOGIES AND CONCEPTS OPERATION, October 2012.

Hung., J.K, Gonzalez L.F. (2012). On parallel hybrid-electric propulsion system for unmanned aerial vehicles", Progress in Aerospace Science, **51**: 1-17.

Leksono E., Haq I. N., Iqbal M. , Soelami FX N.o, Merthayasa IGN., (2013) . State of Charge (SoC) Estimation on LiFePO4 Battery Module Using Coulomb Counting Methods with Modified Peukert. *Joint International Conference on Rural Information & Communication Technology and Electric-Vehicle Technology* (rICT & ICeV-T), November 26-28, Bandung-Bali, Indonesia.

Luyks L. J. (2016). Hybrid Electric Power Helicopter. Patent No. US 9248908, Feb. 2, 2016.

McCormick B.W. (1995). *Aerodynamics, Aeronautics, and Flight Mechanics*, 2nd Ed., J. Wiley and Sons.

Merical K., Beechner T., Yelvington P. (2014). Hybrid-Electric, Heavy-Fuel Propulsion System for Small Unmanned Aircraft. SAE Technical paper, 2014-01-2222.
Nagata H., Chikusa Y., (2014). A lithium sulfur battery with high power density. Journal of Power Souces 264, 206-210.

Su, Y., Liahng, H., and Wu, J., (2008). Multilevel Peukert Equations Based Residual Capacity Estimation Method for Lead-Acid Batteries. IEEE International Conference on Sustainable Energy Technologies, IEEE Publ., Piscataway, NJ, pp. 101–105.

Traub L.W. (2011). Range and Endurance Estimates for Battery-Powered Aircraft, *J. of Aircraft*, **48**(2): 703-707.

Tremblay O., Dessaint L.-A., Dekkiche A.I., (2007). A Generic Battery Model for the Dynamic Simulation of Hybrid Electric Vehicles. IEEE Vehicle Power and Propulsion Conference 0-7803-9761-4/07

Waltner P. J. (2016). Hybrid Electric Power Drive System for a Rotorcraft. Patent No. WO 2016/049027, March 31, 2016

Zhang Y., Wang Y., Wang L., Lo C-M, Zhao Y., Jiao Y., Zheng G., Peng H. (2016). A fiber-shaped aqueous lithium ion battery with high power density. J. Mater. Chem. A, 2016, **4**: 9002-9008.

About the authors

GIULIO AVANZINI (corresponding author) is professor in Flight Mechanics at the University of Salento, Department of Engineering for Innovation, since 2011, teaching Flight Mechanics and Aircraft Design. He graduated in Aeronautical Engineering and earned a Ph.D. in Theoretical and Applied Mechanics from the University “La Sapienza”. He worked for the Italian Ship Model Basin (INSEAN), moving to Politecnico di Torino in 1998, where he served until 2011. Between 2004 and 2012 he spent several semester as visiting professor at Glasgow University and University of Illinois at Urbana Champaign. His research interests span various fields of atmospheric and space flight mechanics, including rotorcraft dynamics, performance of electrically driven aircraft, nonlinear dynamic analysis and control techniques of aerospace vehicles, spacecraft attitude dynamics and control, orbital dynamics.
Email: giulio.avanzini@unisalento.it

TERESA DONATEO is Associate Professor in Fluid Machinery, Energy Systems and Power Generation at the Department of Engineering for Innovation, University of Salento since 2014, teaching courses on Fluid Machinery and Hybrid Electric Powertrains. She attended the School of Material Engineering at the University of Lecce (Italy), and graduated in 1999. In November 2001 she joined the faculty of Engineering at the University of Salento as Assistant professor and in July 2003 received her Ph.D. from ISUFI in the field of Combustion and Energy Conversion. She has been collaborating since 2005 with the Ohio State University, Columbus, OH and since 2001 with major automotive and aircraft industrial partners. She is the author of more than 70 scientific publications mainly focused on simulation, design and optimization of internal combustion engines and hybrid electric powertrains.
Email: teresa.donateo@unisalento.it

ANGELO CARLÀ Angelo Carlà is an undergraduate M.Eng. student in Mechanical Engineering at University of Salento. He obtained a B.Eng degree in Industrial Engineering from the same University in 2013. He is working on the analysis of hybrid powertrains for aeronautical applications for his final project. He is also an intern at CNH Lecce. He is expected to complete his Master course in January 2017.
Email: angelo.carla@studenti.unisalento.it